Factors influencing colour in white Portland cements

D.E. Macphee[1], J.A. Duffy[1] and D. Herfort[2]
[1]University of Aberdeen, Aberdeen, Scotland, UK; [2]Aalborg Portland A/S, R&D Centre, Aalborg, Denmark

1 Introduction

In the increasingly competitive construction materials market, concrete aesthetics have become a significant factor. The architectural flexibility available through colour becomes attainable with the use of white cements which, when suitably treated to limit adhesion of dirt or biofilm growth, can, either by themselves, or when incorporating coloured pigments, provide durable aesthetics. A white concrete substrate offers wider colouring opportunities than conventional concretes so it is important that colouration during white cement manufacture is inhibited. Usually it is the unavoidable presence of iron that is responsible for the faint yellow colouration typically observed in white cements. The actual colour and its intensity depend on the amount and chemical condition of iron, that is, its oxidation state, stereochemistry, and the nature of next or near-next atoms. Here we consider these factors and how they can be interchanged or modified to improve the control of colour in cement making.

A material is coloured if it absorbs electromagnetic radiation in the wavelength range corresponding to visible light (approximately 400 nm to 700 nm, or 25,000 cm^{-1} to 14,000 cm^{-1}). The observed colour is complementary to that absorbed, i.e. the observer sees light (colours) of wavelengths not absorbed by the material. The intensity (or depth) of colour is related to the intensity of absorption, which in turn is related to the concentration, *c* in mol/L, of the absorbing species, its absorbing efficiency (or molar absorptivity, ε) and *l,* the path length (the distance travelled by the light through the material). This relationship is expressed by the Beer Lambert law:

$$\text{Absorbance} = c\varepsilon l \qquad \text{(Eq. 1)}$$

The significance of the oxidation state of iron to the colour of clinker is evident from the absorption spectra for iron [1-3]. Fig. 1 shows that absorption due to ferric ion in an iron-doped Na_2O-CaO-MgO-SiO_2 glass, a matrix with a chemically similar environment to that of a cement clinker, will lead to colouring of the glass (as light with wavelengths in the visible range is absorbed), but absorption due to the ferrous ion does not affect the colour because this mainly occurs outside the visible range (in the infra-red and in the ultra violet regions of the spectrum with little intrusion into the visible region).

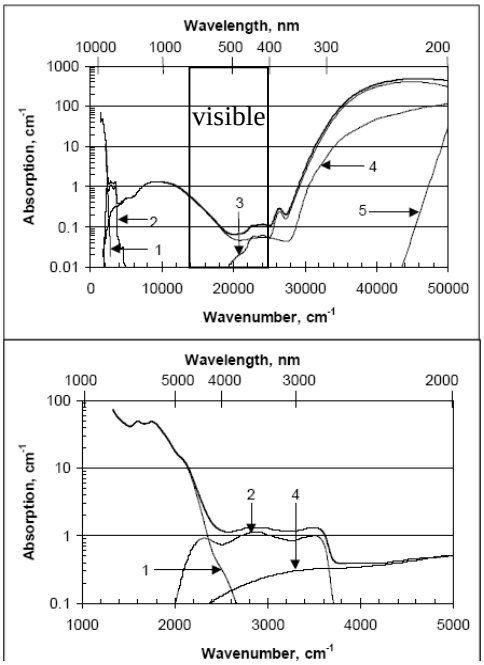

Fig. 1. Absorption spectrum of Fe-doped Na_2O-CaO-MgO-SiO_2 glass (solid line) indicating (1) multiphonon edge, (2) hydroxyl ion, (3) ferric ion, Fe^{3+}, (4) ferrous ion, Fe^{2+}, and (5) L-centre edge contributions (modified from [1]).

The concentration of iron in most white Portland cement clinkers is low (typically only a few wt.%) but this is sufficient to impart a weak discolouration to the clinker making control of whiteness a technological challenge. The focus is therefore on absorption energies and molar absorptivity (from Beer Lambert), both of which are characteristics of bonding environments in the material. The structure and bonding of cement minerals are in turn, conditioned by the processing conditions in the cement kiln so, in principle, there would appear to be a theoretical basis for conditioning colour in cement clinkers by manipulating bonding characteristics in clinker phases.

1.1 Absorption of light in solids

The various mechanisms for absorption of light in the visible region of the electromagnetic spectrum (and hence the development of colour) involve electronic transitions between electron orbitals surrounding metal ions and ligands. These transitions are subject to selection rules (which take account of quantum parameters such as angular momentum and spin). For transition metal compounds (including iron-substituted calcium silicates and/or aluminates), the metal environment is analogous, but not identical, to that obtained in aqueous complexes, i.e. octahedral or tetrahedral co-ordination by oxygen atoms. The principal difference is that essentially, aqueous complexes are isolated structural units in which electronic structures can be described by discrete energy levels whereas in the extended structure of a solid, bonding characteristics are influenced by neighbouring environments due to overlapping electronic orbitals from one ‘structural unit’ to the next. For example, the octahedral aqueous complex, $[Fe(OH_2)_6]^{2+}$, provides a single FeO_6 arrangement but in the solid, the oxide ions are shared with co-ordinating cations (not necessarily Fe^{2+}) in adjacent structural units.

The many Fe^{2+}-O^{2-}, Fe^{2+}-M^{n+}, O^{2-}- O^{2-} interactions lead to a large number of molecular orbitals (bonding and antibonding) of energies so close to each other that they are represented by continuous bands – see Fig. 2. This is the origin of the band theory of solids in which the

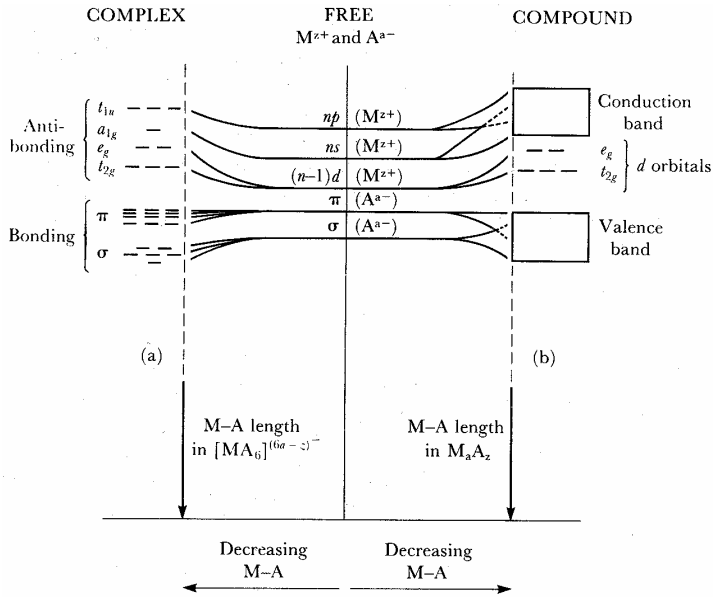

Fig. 2: The effect of decreasing M-A bond lengths in octahedral MA_6 units in the formation of (a) an aqueous complex and (b) a simple solid, reproduced from [4]

valence band corresponds to the lower-energy bonding orbitals (essentially of ligand character) and the conduction band comprises the higher-energy antibonding orbitals (principally of metal character). In the case of coloured solids (of transition metal compounds), the persistence of metal *d*-orbitals allows the possibility of *d-d* transitions.

These *d-d* transitions are intrashell (i.e. they occur within the electronic structure of the atom or ion). They are however, Laporte-forbidden (selection rule related to orbital symmetries) so absorption intensity is weak (molar absorptivity, $\varepsilon < 100$). The Laporte rule can be relaxed by vibrational effects, by the introduction of more covalency in the metal ion–oxygen bond, and by reducing complex symmetry. For example, $[Co(OH_2)_6]^{2+}_{(aq)}$ has a weak pink colour whilst $[CoCl_4]^{2-}_{(aq)}$ is deep blue (ε increases by a factor of 10 to 100). Spin-forbidden transitions are more restrictive and correspond to much lower ε values.

While there is not yet sufficient evidence to discount *d-d* transitions as the cause of the weak colouration of the cement, this weakly absorbing process would nevertheless have minimal effect when the colourant (Fe) is present in only low concentrations. Therefore, it is necessary to investigate alternative explanations for the colour effects in cement.

More intense light absorption arises from various charge transfer (CT) processes. These are electronic transitions from ligand to metal, metal to metal (*inter* metal due to close proximity) or metal to ligand transitions and are unlike *d-d* transitions which are sited on a single atom or ion. An example is given for the chromium III ion in Fig.3 (together with the *d*-d bands). For solids, rather than discrete complex ions, it is often useful to refer to the energy band model. The CT transitions are usually between the valence band (filled σ and π orbitals of ligand character) and either the metal *d*-orbitals situated in the band gap or the empty antibonding orbitals situated in the conduction band (Fig. 4) and involve higher energies than *d-d* transitions (Fig. 3). Their higher ε values (several thousand compared to intrashell transitions) arise because the transitions are Laporte-allowed; a well-known

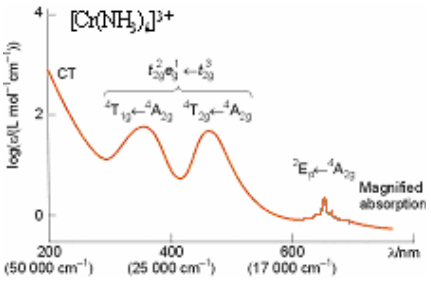

Fig. 3: UV-vis spectrum showing CT peak intensity (at 50,000 cm^{-1} and *d-d* absorbances below 35,000 cm^{-1} for a solution containing hexaammine chromium (III) [5].

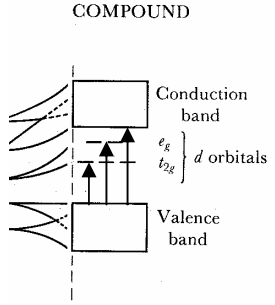

Fig. 4: Possible charge transfer transitions in a solid. Note the difference in transition energies (compared with *d-d*)

examples is $[MnO_4]^-$ from which the intense purple colour is derived from an O^{2-} (ligand) to Mn^{7+} (metal) transition (ε = 2,400 $l.mol^{-1}.cm^{-1}$).

Commonly, CT transitions correspond to UV energies and therefore do not contribute to colour in the solid. However, where the CT transition energies extend into the visible range, intense colours can be observed just as in the case of potassium permanganate, and aqueous Fe^{3+} solutions (yellow). The charge transfer energy is a feature of the tightness of binding of the electron in the region of the metal-ligand bond, a characteristic which defines orbital energies and consequently the band structure for a complex or solid. In oxide systems, the orbitals associated with the oxide ion correspond to energies in the valence band but unlike most other ligand systems, the energies associated with the oxide ion orbitals are variable and strongly dependent on the oxide system concerned. This means that the band structure in oxide systems is correspondingly strongly dependent on composition. This variability in orbital energy reflects variability in the electron binding potential and it is necessary to pursue the concepts of electronegativity and polarisability in order to obtain a quantitative appreciation of the factors which influence colour in oxidic systems.

1.2 Electronegativity and Polarisability.

The strength of interaction between two bonding species is related to the difference in their electronegativities (i.e. their tendancy to bind electrons). In fact, Pauling used formation enthalpies to derive his original electronegativity scale. Examination of *thermochemical* data for oxides systems however shows that oxygen (almost uniquely) does not have a fixed electronegativity. An empirical relationship between oxide ion electronegativity (x_o) and that of the co-ordinating cation (x_M), valid for a range of oxides [4], is given by:

$$x_o = 4.1 - \frac{0.86}{x_M - 0.25} \qquad \text{[Eq. 2]}$$

This variation in electronegativity also correlates with variable effective charge on the oxygen in different oxide systems. It can be shown that a charge approaching –2 is found only in oxides with the most electropositive metals, e.g. K_2O.

These variable characteristics of the oxide ion can also be directly observed from electronic spectra. *Optical* electronegativity, χ_{opt}, more closely reflects the bonding (ionic as well as covalent character) in complexes, due to its origins in established molecular orbital energy structures, and is obtained for individual ions from the lowest energy CT absorption frequency, ν

$$\nu_{max(CT)} = 30{,}000(\chi_{opt(cation)} - \chi_{opt(anion)}) \qquad \text{[Eq. 3]}$$

so that $\chi_{opt(cation)}$ can be calculated from ν for a complex provided $\chi_{opt(anion)}$ is known (and *vice-versa*). An analogous situation exists for solid compounds where, this time, the band gap, E_g is related to χ^*_{opt}:

$$E_g = 3.72[\chi^*_{opt(cation)} - \chi^*_{opt(anion)}] \qquad \text{[Eq. 4]}$$

Slight differences can be found for χ^*_{opt} compared with χ_{opt} derived from spectra of aqueous complexes but these are not great and can be considered to be approximately equal. [If *d-d* spectra are observed in solids, one must consider the position of *d* orbitals in the band gap (Figs. 2 and 4) and the occupancy of the various orbitals.] Although various corrections may be required to accommodate electron spin pairing energies for an electron entering already singly occupied orbitals, the variable optical electronegativity of the oxide ion can be readily observed from spectral data on oxide systems and an equation analogous to [Eq. 2] can be obtained with χ^*_{opt} replacing x, for the same range of oxides (i.e. excluding those in which metal configuration does not correspond to Group 0). This variation in x, χ_{opt} and χ^*_{opt} also extends to polarisability (distortion of the electron charge cloud) of the oxide ion, α_O, which in turn influences the oxide ion's ability to act as an electron pair donor (Lewis base). All of these factors reflect the relative 'floppiness' of electron density around the oxide ion and this is strongly influenced by the polarising power of co-ordinating cations. The stronger the cation influence, the more polarised the electron

density becomes. The polarising ability of the cation is related to it positive charge density:

$$\xi = z^2/d \qquad \text{[Eq. 5]}$$

where z is the nuclear charge and d is the ion diameter. Consequently, the effect of various ions on the polarisability of the oxide ion can be illustrated by the following example (see Fig. 5):

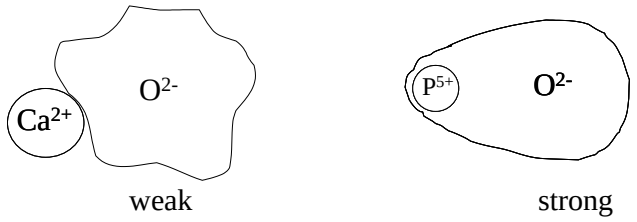

Fig. 5: Effect of cation polarisability on the polarisation of electron density on an oxide ion

2 Relevance to Cement Systems

In binary oxide systems, the polarisation of the oxide ion is influenced by two cations, e.g. in dicalcium silicate, the Ca^{2+} and the Si^{4+} ions have different interactions with the oxide so that the electron density on the oxide ion is averaged between the two influences. When a third component is present, e.g. iron in a calcium silicate phase, the ion (e.g. Fe^{2+} or Fe^{3+}) occupies a cation site. The nature of *its* interaction with oxide ions bridging to adjacent Si tetrahedral sites or Ca sites in a calcium silicate cement phase will therefore be influenced by the average polarisation experienced by that oxide ion due to the combination of neighbouring Si^{4+}, Ca^{2+} and the Fe ion itself. Bearing in mind that the ease of CT between ligand (O^{2-}) and metal (Fe^{n+}) orbitals is influenced by the level of polarisation of the oxide ion's electron density, it now becomes evident that the energy of CT must be variable depending on the combined influences of the Fe^{n+} ion and the neighbouring Si^{4+} *and* Ca^{2+} cations. Not only does this observation offer a means of reconciling electronic spectra with structure and bonding related properties but it also offers a route to influencing energies of transition. The more polarised the electron density of the oxide ion, i.e. the more acidic the environment, the higher the energy required for CT. In the context of cement chemistry, there may be options to make the 'cement' components more acidic. This reduces $\chi^*_{opt(O^{2-})}$ in the co-ordination sphere of the iron and raises the term $[\chi^*_{opt(Fe^{3+})} - \chi^*_{opt(O^{2-})}]$ in Eq. 4, shifting the CT transition into the UV region of the electromagnetic spectrum.

3 Linking optical properties to composition

As we have seen, the value of χ_{opt} for oxide is not fixed, but varies depending on its state of polarisation or basicity. This state can be expressed numerically as the *optical basicity*, which is defined with reference to crystalline calcium oxide having an optical basicity value, Λ, of unity. Originally, the optical basicity scale was arrived at using spectral shifts in the s-p (ultraviolet) spectra of large cations such as Tl^{+} or Pb^{2+} dissolved in silicate, borate, etc. glasses. The data indicated that the optical basicity of an oxidic material could be calculated from its chemical formula using the relationship:

$$\Lambda = \frac{X_{M_A}}{\gamma_{M_A}} + \frac{X_{M_B}}{\gamma_{M_B}} + \ldots \qquad \text{[Eq. 6]}$$

where X_{M_A}, X_{M_B} … are the fractions of positive charge of each metal ion (used for neutralising all the oxides in the formula) and γ_{M_A}, γ_{M_A} …, called "basicity moderating parameters", represent the polarising power of the metal ions. Examples of γ values are: Si^{4+}, 2.10; Al^{3+}, 0.60; Ca^{2+}, 1.00; Na^{+}, 0.905, K^{+}, 0.76. Thus, the optical basicity of Na_2SiO_3 is given by Λ = 0.333/0.905 + 0.667/2.10, i.e. 0.686.

The exact relationship between optical basicity and optical electronegativity is not known. However, since the optical basicity of an oxidic material expresses the (average) degree of negative charge borne by the oxygen atoms (or ions), it is expected that χ_{opt}(oxide) should increase with increasing Λ. A limited quantity of data that is available for copper(II) compounds illustrates this trend (Fig. 6). As far as cements are concerned, it is safe to conclude that increasing the optical basicity of the hosting material will result in a red shift of the absorption band and *vice-versa*. The frequency maximum of the charge transfer band of Fe^{3+} occurs in the ultraviolet region, and the colour arising is owing to the edge of the absorption band encroaching at the violet end of the visible region. The eye usually senses this as a shade of yellow. A decrease in the

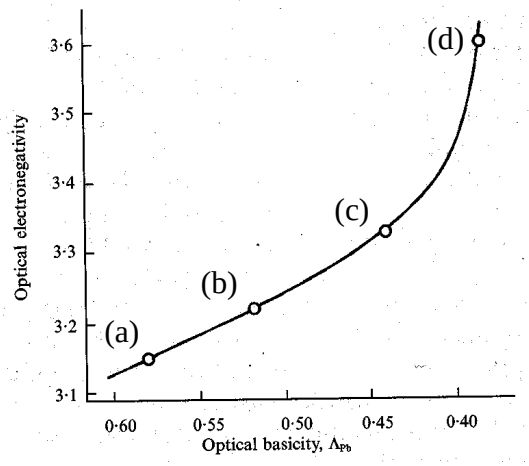

Fig. 6 Plot of optical electronegativity, χ_{opt}, versus optical basicity, Λ, for Cu^{2+} in the following glass environments: (a) Na_2O-B_2O_3 (1:2), (b) Na_2O-P_2O_5 (3:2), (c) Na_2O-P_2O_5 (2:3), (d)AlF_3-CaF_2-SrF_2-MgF_2-SrO-P_2O_5 (7:6:3:2:2:1).

frequency of maximum absorption, effected by increasing optical basicity of the hosting medium, therefore results in further encroachment into the visible region and an increase in the colouration. It follows that in order to minimise the colouring effect of Fe^{3+} it is necessary to encourage the Fe^{3+} into a medium with the lowest optical basicity. In compositional terms, incorporation of more acidic constituents, to more strongly polarise electron density on the oxide ion, may be expected to shift the absorption maximum further into the UV.

4 Application to Model Systems

4.1 Experimental programme

A series of test cement clinkers were prepared from pure materials. Acidic oxides (P_2O_5 $\gamma_{P^{5+}}$ = 2.8 and SO_3 $\gamma_{S^{6+}}$ = 2.8, compared with $\gamma_{Si^{4+}}$ = 2.1) were used as dopants in clinker preparations containing Fe_2O_3 as indicated below. Compositions as defined in Table 1 were mixed and water added to form a paste permitting the formation of nodules, which were then fired at 1450°C, under normal atmospheric conditions. Fired nodules were then ground to 400 m^2/kg, and homogenised.

Table 1. Constituent proportions for base clinker composition (g)

	$CaCO_3$	SiO_2	Al_2O_3
Mix 1	2026	405	0
Mix 2	2493	456	73

Table 2. Mix compositions (g) for spectroscopic study

Sample	Mix 1	Mix 2	Fe_2O_3	P_2O_5	$CaSO_4.$ ½H_2O	SiO_2	$CaCO_3$
1	55						
2	54.8		0.2				0.06
3	54.8		0.2			4.8	0.06
4		54.8	0.2				0.06
5		54.8	0.2			4.3	0.06
6		54.7	0.2	0.15			0.06
7		54.7	0.2		0.2		0.06

The fired products (Mixes 1 and 2; Table 1) were then blended as indicated in Table 2, using water to form pastes. These were then cast into small plastic tubes and allowed to harden over 24 hours. Cylinders were then cut into clinker tablets with a thickness of 15 mm, which were then fired at 1450°C in different oxygen atmospheres according to Table 3.

After cooling/quenching, all samples were characterised for elemental composition by XRF and phase composition was calculated by Bogue (Table 4). C_3S/C_2S ratios were determined by SEM-backscattered electron imaging or by light microscopy. Iron lost by exsolution, if evident, was accounted for on the basis of EDS measurements on

exsolved material. Selective dissolution by KOSH [6] and SAE (same procedure as described in [7] for the SAM method, but where methanol is replaced by ethanol) solutions of the clinkers was undertaken to enable comparison between elemental distributions in silicate and aluminate phases respectively. Diffuse reflectance spectra were obtained using a Minolta CM-3610d spectrophotometer (2º observer, C65 illuminant) at intervals of 10 nm on samples ground to < 45 μm and converted to absorbance data by the following relationship, $A = (1-R(\lambda))^2/2R(\lambda)$, where $R(\lambda)$ is the fraction of light reflected at the wavelength in question relative to MgO.

Table 3. Furnace atmosphere during firing of model clinkers

	Oxygen content (%) in nitrogen			
Sample	0	0.5	3	20
1		+		
x.1	+			
x.2		+		
x.3			+	
x.4				+
x.5	+			
x.6		+		
x.7			+	
x.8				+

x refers to the sample number in Table 2; x.1-x.4 are rapidly cooled in a water bath (quenched); x.5-x.8 are slowly cooled in atmospheric air.

4.2 Results and Discussion

The Bogue phase contents of the high C_2S and high C_3S clinkers are shown in Table 4. The reason for preparing both high and low C_3S clinkers was that the distribution coefficients of iron between all 3 phases (C_3S, C_2S and C_3A) can be assumed to be the same in both samples burned and cooled under the same conditions. This can be used to give a unique solution for the absolute contents of iron in each phase. We have made no distinction here between Fe^{2+} and Fe^{3+}.

Table 4. Bogue composition of synthesised clinkers

(a) high C_2S (Sample 5)	clinker	Insoluble residue after removal of C3A (KOSH)	Concentration of Fe2O3 in each phase
C3S	22.1	20.0	0.41
C2S	64.5	74.4	0.17
C3A	9.6	1.9	1.30
Free lime	2.1	2.1	0.41
(b) high C_3S (Samples 4, 6 and 7)			
C3S	66.2	72.2	0.34
C2S	16.8	18.4	0.14
C3A	10.1	2.3	1.1
Free lime	6.0	4.3	0

The Bogue compositions of the insoluble residues (silicates + free lime), after removal of the C_3A by the KOSH solution, are also shown in Table 4. Approximately 2% C_3A remains, corresponding to the amount of alumina incorporated in the silicates. The mean P_2O_5 and SO_3 contents of the silicates were determined directly from the insoluble residues after KOSH treatment. Then, using the contents of SO_3 and P_2O_5 in the original samples, the contents in the C_3A phase (removed by KOSH) were obtained by subtraction. However, it should be noted that this latter step introduces a rather higher degree of uncertainty in the data. The target SO_3 content in the samples was 0.2%, but clearly significant sulphur has volatilised, particularly at the lower oxygen pressures.

Table 5. Mean P_2O_5 and SO_3 contents of P_2O_5 and SO_3-doped clinkers

	Mean oxide content (%) in silicates (*background*)	
	Sample 6 P_2O_5 (*0.01*)	Sample 7 SO_3 (*0.02*)
Burned in air and cooled slowly in air	0.32 (*0.29*)	0.13 (*0.18*)
Burned in air and quenched at 1100ºC	0.28 (*0.25*)	0.12 (*0.13*)
Burned and cooled to 1100ºC at 3% O_2 then quenched	0.01 (*0.24*)	0.13 (*0.11*)
Burned and cooled to 1100ºC at 0.5% O_2 then quenched	0.31 (*0.28*)	0.07 (*0.07*)
Burned and cooled to 1100ºC at 0% O_2 (100% N_2) then quenched	0.28 (*0.25*)	0.05 (*0.09*)

The absorption spectra for these samples under the various burning and cooling conditions indicated are presented in Fig. 7.

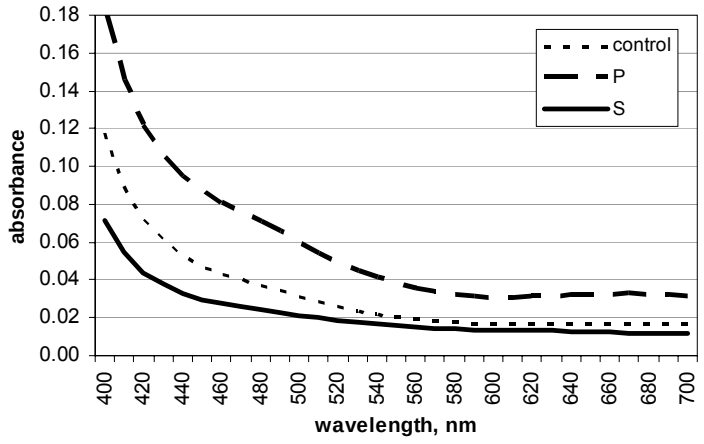

Fig. 7a. Absorbance spectra for SAE insoluble residue (mainly C_3A), samples burned and cooled in air.

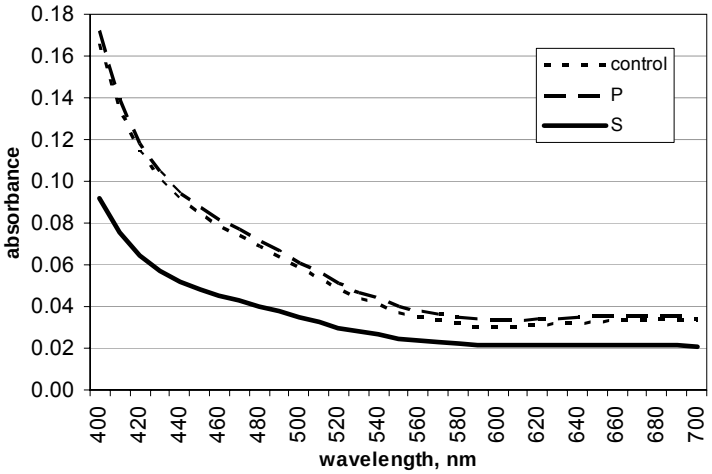

Fig. 7b. Absorbance spectra for KOSH insoluble residue (mainly C_3S), samples burned and cooled in air.

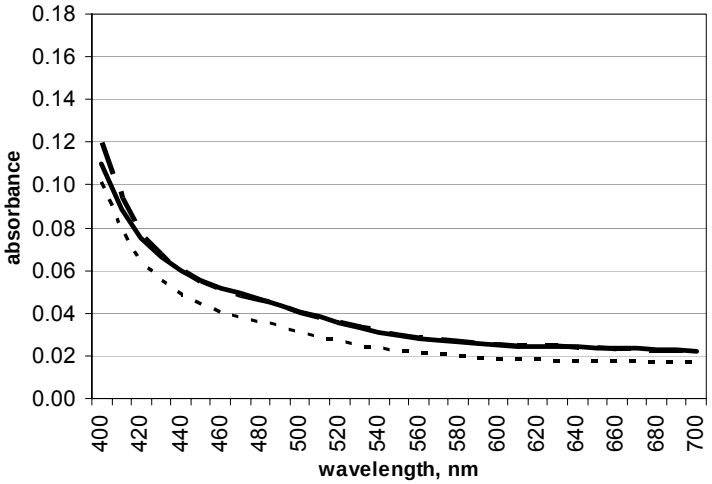

Fig. 7c. Absorbance spectra for KOSH insoluble residue (mainly C_3S), samples burned at 0% O_2 and quenched in water.

It is apparent from these results that S^{6+} shifts the absorption towards the UV region for both the silicate and aluminate phases under the most oxidising condition where the samples were burned and cooled in air (fig. 7a and b). However, this effect was not apparent under more reducing condition (fig 7c). This is encouraging since the acidity of S^{6+} ($\gamma_{S^{6+}}$ = 2.8) would be considered to be strongly polarising of the oxide ion electron cloud and its effect on colour implies that the S^{6+} ion is located in the vicinity of the Fe^{3+}-O^{n-} bond, particularly as the bulk sulphur concentration is rather low (Table 5). It is significant to note, however, that P^{5+}, having the same acidity as S^{6+}, was not as effective, at least in the silicate phases burned and cooled air, and consequently,

it may be inferred that P^{5+} is not accumulating in the vicinity of the Fe^{3+}-O^{n-} bond.

Even though oxidation of Fe^{2+} to Fe^{3+} probably results from the oxygen-rich atmosphere, the dominant effect is the shift of the absorption maximum by the introduction of acidic components, as predicted, which apparently accumulate in the vicinity of the Fe^{3+} chromophore. It is noted also that under less oxidising conditions, reduced effect may be attributable to the lower sulphur contents but this requires further study. In any event, the oxidising conditions seem to be important and may stabilise the S (VI) oxidation state of sulphur.

5. CONCLUSIONS

A model based on electronic structures of oxide systems has been presented to explain colour effects in white Portland cements. The polarisability of electron density on oxide ions and in metal oxide bonds can be directly associated with light absorption such that composition can be modified to influence colour in oxidic materials (e.g. cements). To test the model, this preliminary study has shown that colour effects due to Fe^{3+} in white cement can be reduced by the introduction of acidic oxides. In this case, S^{6+}, introduced as SO_3, has shifted frequency of maximum absorption attributed to Fe^{3+}, further into the UV region of the electromagnetic spectrum. Although P^{5+} exhibits similar acidity to S^{6+}, it was unable to consistently reduce absorbance in the visible range of the spectrum. This study has therefore highlighted the importance of colour modifying oxides both in terms of their acidity and in terms of distribution relationships with chromophores in cement phases. To achieve colour reduction, S^{6+} appears to have located in the region of the Fe^{3+}-O^{n-} bond, a situation not evident in P-doped clinkers.

6. REFERENCES

[1] L. Glebov and E. Boulos, 'Absorption Spectra of Iron and Water in Silicate Glasses', *ICG 2000*, (Amsterdam); 'Glass in the New Millenium'.

[2] E.N. Bouloe, L.B. Glebov and T.V. Smirnova, 'Absorption of iron and water in the Na_2O-CaO-MgO-SiO_2 Glasses. Part 1. Separation of the Ferrous and Hydroxyl Spectra in the Near IR Region', J. Non-Cryst. Solids, 221, (1997), 213

[3] L.B. Glebov , E.N. Boulos, 'Absorption of iron and water in the Na_2O-CaO-MgO-SiO_2 Glasses. II. Selection of intrinsic, ferrous and ferric spectra in the visible and UV regions'. J Non-Cryst. Solids, 242 (1998), 49-62.

[4] J.A. Duffy, 'Bonding, Energy Levels and Bands in inorganic solids' (Longman, 1990), p107 and Chapter 6.

[5] D.F. Shriver and P.W. Atkins, Inorganic Chemistry, 3rd Ed., (Oxford University Press, 1999), p438

[6] W.A. Gutteridge, 'On the dissolution of the interstitial Phases in portland Cement'. Cement and Concrete Research, Vol. 9, pp. 319-324, 1979

[7] L. Hjort and K.G. Lauren, "Belite in Portland Cement'. Cement and Concrete Research, Vol. 1, pp. 27-40, 1971.